Published online April 20, 2005

Quantifying Ground Water Inputs along the Lower Jordan River

Ran Holtzman, Uri Shavit,* Michal Segal-Rozenhaimer, Ittai Gavrieli, Amer Marei, Efrat Farber, and Avner Vengosh

ABSTRACT

The flow rate of the Lower Jordan River has changed dramatically during the second half of the 20th century. The diversion of its major natural sources reduced its flow rate and led to drying events during the drought years of 2000 and 2001. Under these conditions of low flow rates, the potential influence of external sources on the river discharge and chemical composition became significant. Our measurements show that the concentrations of chloride, calcium, and sodium in the river water decrease along the first 20-km section, while sulfate and magnesium concentrations increase. These variations were addressed by a recent geochemical study, suggesting that ground water inflow plays a major role. To further examine the role of ground water, we applied mass-balance calculations, using detailed flow rate measurements, water samplings, and chemical analyses along the northern (upstream) part of the river. Our flow-rate measurements showed that the river base-flow during 2000 and 2001 was 500 to 1100 L s^{-1}, which is about 40 times lower than the historical flow rates. Our measurements and calculations indicate that ground water input was 20 to 80% of the river water flow, and 20 to 50% of its solute mass flow. This study independently identifies the composition of possible end-members. These end-members contain high sulfate concentration and have similar chemical characteristics as were found in agricultural drains and in the "saline" Yarmouk River. Future regional development plans that include the river flow rate and chemistry should consider the interactions between the river and its shallow ground water system.

Water resources in arid and semiarid regions are often overexploited. Many rivers in these regions become saline and polluted, and their low flow rates further endanger their future sustainability (Pillsbury, 1981; Williams, 2001). The Lower Jordan River is an extreme example of such a river, where the combination of excessive water needs and lack of environmental attention has led to a devastating drying process of the river (Salameh, 1996).

Over the last 50 years the flow rate of the Lower Jordan River has decreased from about 1300×10^6 m^3 yr^{-1} at the outlet to the Dead Sea to very low flow rates, recently estimated around 100 to 200×10^6 m^3 yr^{-1} (Salameh and Naser, 1999). The historical main tributaries included the Upper Jordan River flowing through the Sea of Galilee (approximately 540×10^6 m^3 yr^{-1}), the Yarmouk River (approximately 480×10^6 m^3 yr^{-1}), and local streams (Hof, 1998). Since the construction of water supply projects in Israel (mainly since 1964), Jordan (1966), and Syria (1970), the Sea of Galilee and the Yarmouk River are blocked and no fresh surface water flows into the river except for rare flood events and negligible contributions from small springs.

The influence of natural ground water seepage and agricultural return flows were negligible relative to the historical flow rates of the Lower Jordan River. However, both sources became potentially significant following the sharp decrease in the river flow and the growing agricultural activity along its banks. In an earlier paper (Farber et al., 2004) we used the geochemical variations to show that the river chemistry is primarily controlled by ground water contribution (including agricultural return flows) and that surface inputs alone cannot account for the overall chemical changes. In the present study, we quantify the ground water contribution by an integration of flow rate measurements with the chemical changes that were observed along the Lower Jordan River.

MATERIALS AND METHODS

We present results of flow-rate measurements, chemical analyses, and mass-balance calculations along the upper (northern) 20 km of the Lower Jordan River. The results were obtained in collaboration between Jordanian, Israeli, and Palestinian researchers between 1999 and 2001. The rainfall during these years was limited (approximately 75% of the annual average) and thus the reported results represent base flows under drought conditions.

The Study Area

The Lower Jordan River stretches between Alumot dam (downstream from the Sea of Galilee, 32°42′ N, 35°35′ E, approximately 210 m below sea level) and the Dead Sea (31°47′ N, 35°33′ E, approximately 417 m below sea level in 2004) with a catchment area of about 15 000 km^2 (Efrat, 1996; Salameh, 1996; Hamberg, 2000). The river is about 105 km long (aerial distance; approximately 190 km meandering distance; Hamberg, 2000) and defines the border between Israel and Jordan. This paper focuses on the northern part of the Lower Jordan Valley (see Fig. 1, Table 1), between Dalhamia (Site 7) and Hamadia pumping station (Site 25). The investigated area is occupied by rural settlements on both sides of the river and the majority of the land is used for agriculture (e.g., field crops, date plants, and fishponds). Tributaries to the river include natural streams and artificial canals (e.g., agricultural and fishpond drainage). Currently, the only major water sources at the inlet of the Lower Jordan River are the Saline Water Carrier and the effluents from the Bitania wastewater treatment plant (Sites 1 and 2). The Saline Water Carrier contains a mixture of saline spring water diverted from the western shore of the Sea of Galilee and treated urban sewage effluents. The Bitania source consists of poorly treated waste effluents.

R. Holtzman, U. Shavit, and M. Segal-Rozenhaimer, Department of Civil and Environmental Engineering, Technion, Israel Institute of Technology, Haifa 32000, Israel. I. Gavrieli, Geological Survey of Israel, 30 Malkhe Israel Street, Jerusalem 95501, Israel. A. Marei, Faculty of Science and Technology, Al-Quds University, P.O. Box 20002, East Jerusalem. E. Farber and A. Vengosh, Department of Geological and Environmental Sciences, Ben Gurion University, PO Box 653, Beer Sheva 84105, Israel. Received 26 June 2004. Technical Reports. *Corresponding author (aguri@technion.ac.il).

Published in J. Environ. Qual. 34:897–906 (2005).
doi:10.2134/jeq2004.0244

677 S. Segoe Rd., Madison, WI 53711 USA

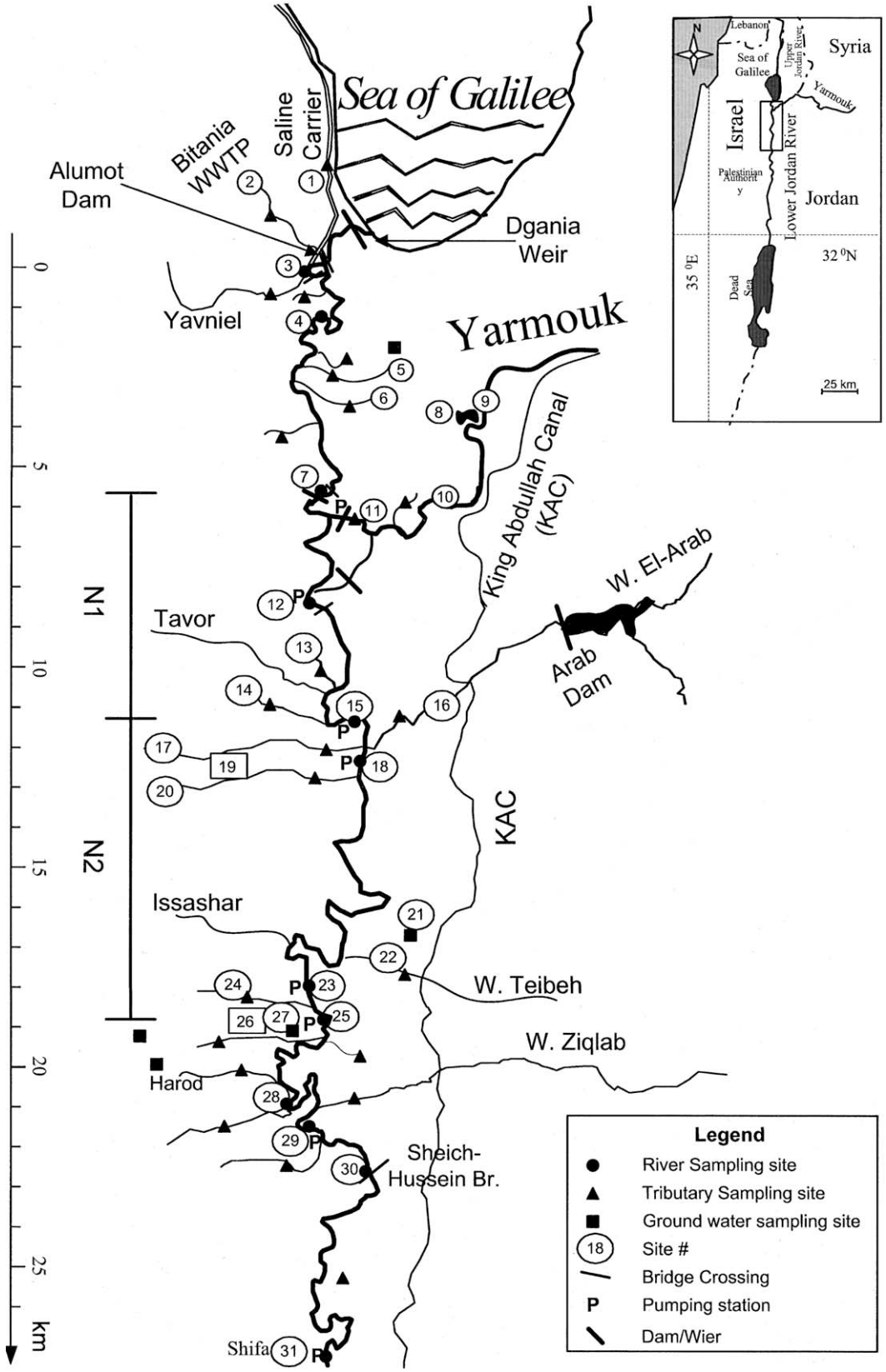

Fig. 1. The northern part of the Lower Jordan River (sites are listed in Table 1).

Table 1. Sites list (for location see Fig. 1).

Site	Name	Aerial distance from Site 3	Type†
		km	
1	Saline Carrier	0	W
2	Bitania	0	W
3	Alumot	0.1	JR
4	Beit-Zera Bridge	1.3	JR
5	Kohvani Drainage	2.5	D
6	Afikim Drainage	3.4	D
7	Dalhamiya bridge	5.6	JR
8	Yarmuchim Reservoir	3.3	E
9	Yarmouk (121)	3.5	E
10	Yarmouk (110)	3.7	E
11	Saline Yarmouk	6.3	E
12	Gesher	8.7	JR
13	D. Canal Gesher	10.7	W
14	D. Canal Neve-Ur	11.5	W
15	Neve-Ur N.	11.6	JR
16	W. El-Arab	12.2	E
17	D. Canal 76	12.2	W
18	Neve-Ur S.	12.7	JR
19	Nave-Ur fishpond	12.5	F
20	Fishpond Pipe	12.7	W
21	Manshieh	16	GW
22	W. Teibeh	16.5	E
23	Hamadiya N.	18.2	JR
24	Doshen Canal	18.5	W
25	Hamadiya S.	19.5	JR
26	Hamadiya Fishponds	19.1	F
27	Hamadiya Well	19.1	GW
28	Gate 48	21.1	JR
29	Maoz Hayim	22.2	JR
30	Shiech-Hussein Bridge	22.7	JR
31	Shifa	27.7	JR

† JR, Jordan River sites; W and E, western and eastern tributaries (streams and drainage canals); GW, ground water sampling through boreholes, wells, or springs; D, agricultural draining canals; F, fishponds.

Water Sampling and Chemical Analysis

The waters of the Lower Jordan River and its tributaries were sampled between August 1999 and August 2001. Water samples were also collected from fishponds, agricultural drainage canals, and different subsurface sources.

Sampling was obtained at various locations along the selected cross-sections, representing cross-sectional averages with occasionally unavoidable potential bias toward the upper water layers. Water samples were collected in rinsed plastic bottles, filtered (0.45 μm) within 24 to 48 h, stored at 4°C, and finally analyzed at the Israel Geological Survey. While concentrations of chloride and sulfate (among other anions) were measured by ion chromatography (IC), concentrations of sodium and calcium were measured by inductively coupled plasma–optical emission spectrometry (ICP–OES). The imbalance between positive and negative charged ions did not exceed 5%, which reflects the overall precision of the analytical procedures. Isotope ratios of sulfur in sulfate were also determined. For $\delta^{34}S$ analyses, SO_2 gas was produced and collected on a vacuum line as described by Coleman and Moore (1978) (Gavrieli et al., 2001). Isotopic measurements of the SO_2 gas were done at the British Geological Survey, Keyworth, UK. For more chemical and isotope analyses obtained for these water samples, see Segal-Rozenhaimer et al. (2004) and Farber et al. (2004).

Flow Rate Measurements

Flow rates were measured during five field trips between February and August 2001 at three river cross-sections along the northern part of the Lower Jordan River, and in the eastern and western tributaries (adjacent to their confluence with the river). These measurements were obtained simultaneously with the water samplings designated for the chemical analyses. The duration of each field trip was 1 to 2 d (except for the February field trip during which the tributaries were measured a week later). The flow-rate measurement technique was adjusted according to the local conditions. In particular, because the river centerline serves as the international border between Israel and Jordan, the research team was not allowed to cross the river and a special measurement procedure was developed. A portable acoustic Doppler velocimeter (Argonaut-ADV; Sontek, San Diego, CA) was mounted on a vertical pole held by a specially designed floating traverse construction (Fig. 2). By cruising the construction across the river using magnesium-alloy poles, both water velocity and riverbed profiles were obtained. The immersion depth of the instrument was adjusted using a step motor and a control cable, and measured by an internal pressure gauge (±1 cm). The instrument orientation and lateral location were recorded using internal compass, tilt

Fig. 2. A picture of a discharge measurement site showing the acoustic Doppler velocimeter (ADV) mounted on the floating construction. A schematic of the floating construction and the ADV is shown on the right.

sensors, and a ruler that was attached to the magnesium poles (±5 cm). A portable computer and serial communication were used for instrument control and data recording. The three-component velocity vector was measured with a high signal-to-noise ratio thanks to the high turbidity of the river (approximately 60 NTUs). The measurement of the riverbed profile utilized the boundary reflection signal and the ability of the instrument to separate it from the velocity signal. The estimated relative accuracy of the measured water depth and cross-section width in the river sections was 5 and 2%, respectively (Holtzman, 2003). The ADV was programmed to measure the velocity vector 2000 to 10 000 times (at a frequency of 10 Hz) within its approximately 0.25-cm^3 sampling volume for each point, resulting in an estimated relative accuracy of approximately 1% (Sontek, 2000). Post-processing was applied to remove measurements with temporary low signal-to-noise ratio before an average value was obtained.

An electromagnetic velocimeter (Flo-Mate Model 2000; Marsh-McBirney, Frederick, MD) was used to measure velocities in the western tributaries, while a dipping bar (Hydro-Bios, Kiel, Germany) was applied in the eastern tributaries. Velocity was measured with the electromagnetic velocimeter 5 to 10 times at each point (5 s each) with a sampling frequency of 30 Hz (a total of 750 to 1500 measurements at each point). The accuracy of the electromagnetic velocimeter measurements was estimated as 2% with a 1.5 cm s^{-1} zero offset induction (Marsh-McBirney, 1990). The accuracy of the dipping bar measurements was estimated as 20% (J. Von-Borries, personal communication, 2003).

Flow rates were obtained by an integration of the scalar product between the velocity vector and the cross-sectional area vector at 30 to 50 points across each cross-section of the river and 5 to 20 points at the tributaries (Holtzman, 2003, Fig. 20, p. 44). It was found that for most cases, velocity vertical profiles fit a power law, $u(z) = \alpha z^m$, where u (m s^{-1}) is the velocity component perpendicular to the cross-section, z(m) is the height from the riverbed, and α and m are constants. These constants were calculated using linear curve fit procedure from the measurements in each cross-section. For each cross-section, a choice was made between an integration of the power law:

$$Q = \sum_{j=1}^{n}\left[\left(\int_{z=0}^{z=H_j} \alpha_j z^m \mathrm{d}z\right) b_j\right] \quad [1]$$

and a simple two-dimensional integration scheme:

$$Q = \sum_{j=1}^{n}\sum_{k=1}^{K}\left(u_{j,k} h_{j,k} b_j\right) \quad [2]$$

which provided a better fit for a few river cross-sections and for all the tributaries than Eq. [1]. Here j is the column index, n is the number of columns, k is the cell index, $h_{j,k}$(m) is the cell height, and K is the number of cells within the column, b_j(m) is the width of the column, and H_j(m) is its height. The accuracy of measurements of the cell height and width in the tributaries was estimated as 5 and 2%, respectively. The potential error generated by Eq. [1] and Eq. [2] was calculated by a linear approximation. These errors are 5 to 6% for the river flow, 19% for the western tributaries, and 29% for the eastern tributaries (Holtzman, 2003).

RESULTS AND DISCUSSION

River Chemistry

The chemistry of the Lower Jordan River has coherent and repeatable trends along its flow course. The chloride concentration, which decreases along the northern part of the river, is shown in Fig. 3a. Its high initial salinity is due to the discharge of the Saline Water Carrier. Sodium and calcium concentrations also decrease along the northern part of the river (but increase together with chloride along its southern part). Sulfate (Fig. 3b) and magnesium concentrations monotonically increase throughout the river flow path.

In Farber et al. (2004) we presented analyses of water samples collected from the river and its surroundings. Geochemical considerations indicated that the chemical and isotopic compositions of surface tributary inflows could not account for the chemical and isotopic modifications observed in the river. For example, the tributary inflows have higher $^{87}Sr/^{86}Sr$ (western and eastern tributaries) and lower SO_4/Cl ratios (western tributaries) when compared with the river water. Thus, an additional subsurface source has been proposed. The chemical and isotopic variations recorded in the Lower Jordan River suggest that this ground water source has high Na/Cl, high SO_4/Cl, low $\delta^{34}S_{sulfate}$, and low $^{87}Sr/^{86}Sr$ values. Indeed, the mass-balance calculations presented hereafter indicate that subsurface inflows change the chemical distributions along the river.

As a first approximation, we assume that mixing between two distinct water bodies influences the river chemistry; these are the river water at its origin and ground water discharge into the river. We posit that chloride and sulfate are conservative constituents in the river system and show in Fig. 4 that the postulated mixing process leads to an approximately straight line when plotting one conservative constituent versus the other (see line A–B in Fig. 4). The assumption that sulfate is a conservative constituent deserves some attention. Sulfate can be removed from water by reduction to sulfide under anaerobic conditions or by gypsum precipitation if the water is supersaturated with respect to gypsum. Sulfate can also be added to the water by oxidation of organic matter, although the amount of sulfide that is generated from organic matter (e.g., amino acids) that is oxidized to sulfate is low (Hvitved-Jacobsen, 2002). Anaerobic reduction of sulfate in the Lower Jordan River is not likely because the river water along the northern section has dissolved oxygen content of 1 to 10 mg L^{-1} (10 to 100% saturation, Segal-Rozenhaimer et al., 2004), whereas bacterial reduction of sulfate requires total lack of oxygen (Hvitved-Jacobsen, 2002). It is possible that the large content of organic matter within the Jordan River sediments (Segal-Rozenhaimer et al., 2004) results in in situ anaerobic reduction of sulfate, but because the majority of the water volume in the river is under oxidizing condition, it is less likely that the overall sulfate budget will be influenced by these processes. Moreover, the $\delta^{34}S$ values of the Jordan River decrease along the river flow (Farber et al., 2004), therefore excluding the possibility of sulfate reduction. To evaluate the potential precipitation we calculated the saturation level in the Lower Jordan River with respect to gypsum by using the Davis equation that is based on the Debye–Huckel equation (Benjamin, 2002). Our results indicate that the maximum ion activity product is 1.04×10^{-4}

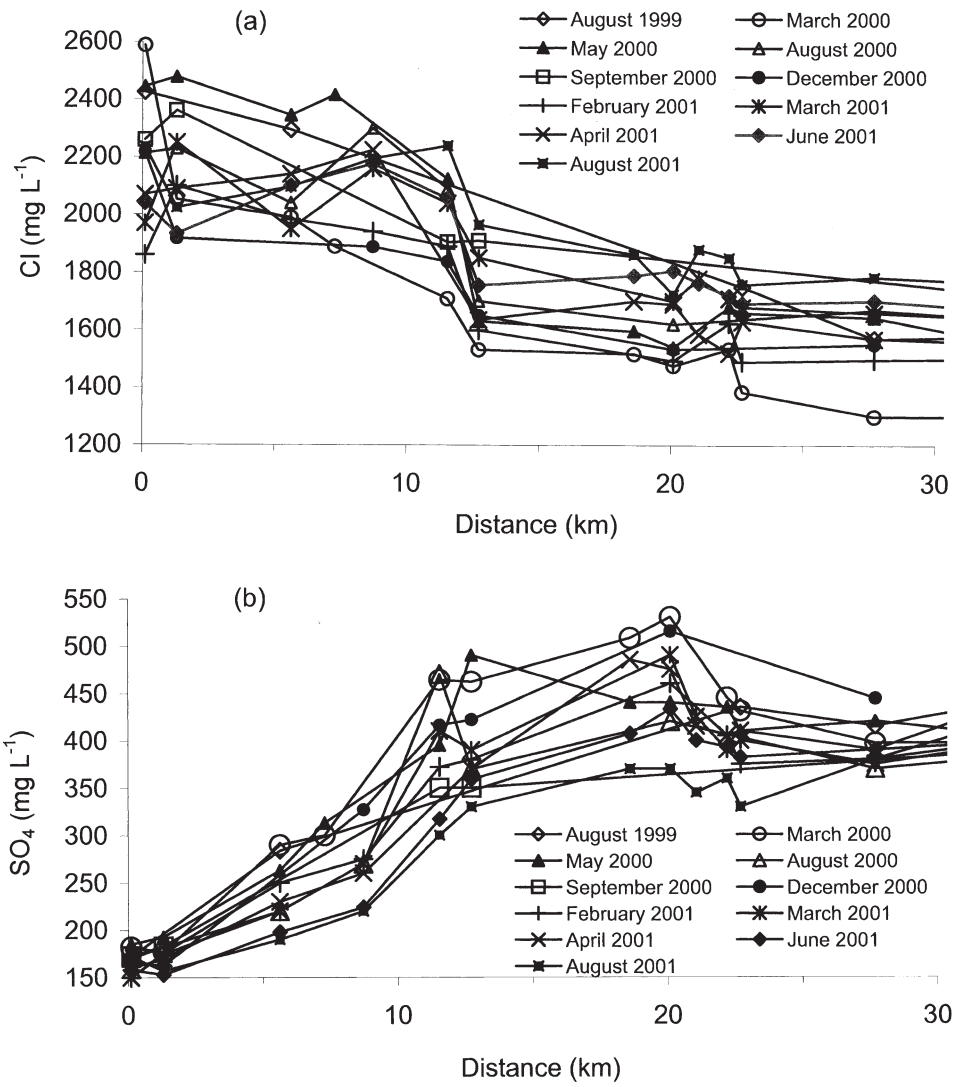

Fig. 3. (a) Chloride and (b) sulfate concentrations along the northern (upstream) part of the Lower Jordan River.

whereas the solubility product (K_{sp}) is 1.22×10^{-4}. Because the Lower Jordan River is undersaturated with respect to gypsum, sulfate removal by precipitation is not likely to occur.

Flow Rate Measurements and Mass-Balance Calculations

The base flows that we measured during the drought years of 2000–2001 (500–1100 L s^{-1}) are about 40 times lower than the historical flow rates. These discharge values are even lower than recent published estimates (e.g., Al-Washah, 2000). While the intensive water use by the regional countries is responsible for the general discharge decrease, drought conditions reduce it further, resulting in local drying events. Such low flow rates increase the potential influence of tributaries and ground water inflows on the river chemistry.

Water-balance calculations were conducted using the flow rates measured at the inlets and outlets of different segments of the river, the measured and reported pumping rates, and reported evapotranspiration. Zero rainfall was reported during and several days before the measurements. The water-balance equation is written as follows:

$$\frac{\partial \forall}{\partial t} = \sum_{i=1}^{n_{(in)}} Q_{in,i} - \sum_{i=1}^{n_{(out)}} Q_{out,i} + \int_{x_1}^{x_2} q_{in}(x)\mathrm{d}x - \int_{x_1}^{x_2} q_{out}(x)\mathrm{d}x - \int_{x_1}^{x_2} B'(x)\,\mathrm{ET}(x)\mathrm{d}x \quad [3]$$

where $Q_{in,i}$(m^3 s^{-1}) and $Q_{out,i}$(m^3 s^{-1}) are the measured flow rates at inlet and outlet i with $n_{(in)}$ such inlets and $n_{(out)}$ such outlets (including pumping stations), $q_{in}(x)$ and $q_{out}(x)$ are the distributed recharge and discharge (flow rate per unit river length, m^2 s^{-1}) along a segment stretching between x_1(m) and x_2(m), $\forall$(m^3) is the water volume of the segment, $B'(x)$ is the effective width (m) for evapotranspiration that includes the vegetation influence, and ET(x) is the rate of evapotranspiration (flow rate per unit area, m s^{-1}). When assuming steady-state conditions ($\partial\forall/\partial t = 0$) and zero distributed outflow [$\int_{x_1}^{x_2} q_{out}(x)\mathrm{d}x = 0$], the total flow rate of the ground water

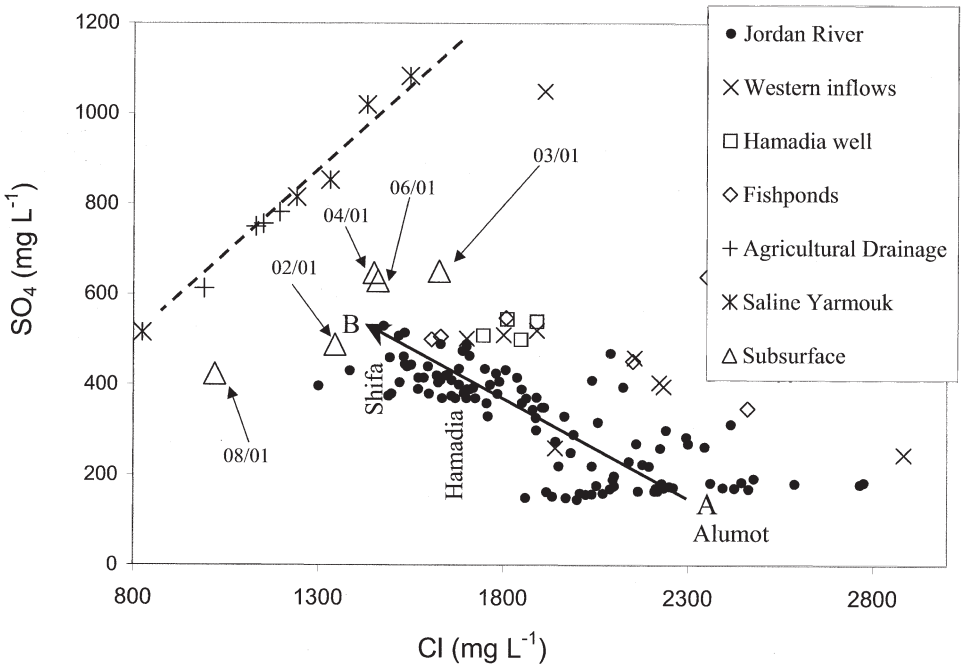

Fig. 4. Sulfate versus chloride concentration in the northern part of the Lower Jordan River and in adjacent sources. Three groups of waters are represented: (i) river water (arrow A and B indicates down-river direction), (ii) sources that represent potential end-members, and (iii) results of the mass-balance calculation [named "subsurface"] representing the chemical composition of the subsurface contribution along N2. Note that "western inflows" are Sites 13, 14, 17, and 24, "fishponds" are Sites 19 and 26, "drainages" are Sites 5 and 6 and Saline Yarmouk is Site 11 (Fig. 1, Table 1). The dates of the measurement campaigns are marked near the "subsurface" results.

contribution [$\int_{x_1}^{x_2} q_{in}(x)dx$, referred to as Q_{gw}(m^3 s^{-1})] can be calculated. The assumption of steady-state conditions was postulated because detailed water-level measurements were not available during most of the discharge measurement campaigns. The possible deviation from steady-state conditions was estimated and then integrated into the error estimation presented below. A few available water-level measurements in nearby observation wells support the zero distributed outflow assumption as they indicate that the head of the ground water adjacent to the river is higher than that of the river. It should be noted that during the study no heavy rain or flood events took place, reducing the likelihood of a reverse flow from the river into the ground water system.

Table 2 shows a list of the total flow rates (L s^{-1}) measured in the N2 segment (Fig. 1). The terms Q_{15}(L s^{-1}) and Q_{25}(L s^{-1}) represent the measured flow rate of the river at the inlet and outlet of the segment. The other flow rates represent tributaries, pumping stations, and evapotranspiration (relatively small). The pumping rates were measured and reported by the local water authorities. The evapotranspiration was calculated using measurements obtained by the Israeli Meteorological Service (personal communication, 2001) in the nearby Eden farm (3.0, 5.1, 5.3, 6.5, and 6.9 mm d^{-1} in February, March, April, June, and August 2001, respectively) and an average effective width of 25 m (Holtzman, 2003). The resulting evapotranspiration values are similar to published records (Salameh, 1996; Hamberg, 2000; Orthofer et al., 2001).

Table 2. Measured discharge and the result of the water mass-balance calculations along the N2 river segment (between Sites 15 and 25; see Fig. 1) of the five measurement campaigns. Inflow is marked as positive.

Term†	Site	February 2001	March 2001	April 2001	June 2001	August 2001
		L s^{-1}				
Q_{15}	Neve-Ur (North)	839	967	862	1087	808
$Q_{15,p}$	Neve-Ur Pump (N)	−160	−233	−231	−243	−276
Q_{16}	Wadi El Arab	160	165	165	85	45
Q_{17}	Drainage Canal 76	0	0	49	50	0
$Q_{18,p}$	Neve-Ur Pump (S)	−80	−80	−49	−104	−97
Q_{20}	Fish Pond Outlet	0	0	0	270	0
Q_{22}	Wadi Teibeh	18	30	30	0	9
$Q_{23,p}$	Doshen Pumps	−244	0	−231	−252	−267
Q_{24}	Doshen Canal	87	12	13	13	0
$Q_{25,p}$	Zor Pumps	−167	−125	−118	0	0
Q_{25}	Hamadia	−1109	−984	−787	−1073	−480
ET (N2)	evapotranspiration	−15	−25	−26	−32	−34
Q_{gw} (N2)	mass-balance results	671	274	323	200	292

† The terms Q_{15} and Q_{25} represent the measured flow rate of the river at the inlet and outlet of the segment. The other flow rates are of tributaries, pumping stations, and evapotranspiration.

Table 3. Measured discharge and the result of the water mass-balance calculations along the N1 river segment (between Sites 7 and 15; see Fig. 1) of the five measurement campaigns. Inflow is marked as positive.

Term†	Site	February 2001	March 2001	April 2001	June 2001	August 2001
		L s^{-1}				
Q_7	Dalhamiya Bridge	671	921	757	659	676
Q_{11}	Saline Yarmouk	183	178	162	0	0
$Q_{11,p}$	Saline Yarmouk Pump	−187	−125	−89	0	0
$Q_{12,p}$	Gesher Pumps	−123	−122	−109	−102	−102
Q_{13}	D. Canal Gesher	68	155	122	79	9
Q_{14}	D. Canal Neve-Ur	31	21	44	222	5
Q_{15}	Neve-Ur (North)	−839	−967	−862	−1087	−808
ET (N1)	evapotranspiration	−8	−14	−14	−18	−19
Q_{gw} (N1)	mass-balance results	205	−48	−11	246	239

† The terms Q_7 and Q_{15} represent the measured flow rate of the river at the inlet and outlet of the segment. The other flow rates are of tributaries, pumping stations, and evapotranspiration.

The ground water contribution (Q_{gw}) was calculated by the mass-balance equation (Eq. [3]), and is shown at the bottom of the table. The same calculations, performed between Sites 7 and 15, referred to as N1 segment (Fig. 1), are presented in Table 3. In most of the periods, Q_{gw} was about 200 to 240 L s^{-1} along N1 segment (approximately 9.5-km meandering length) and 200 to 670 L s^{-1} along N2 segment (approximately 17 km). These contributions constitute 20 to 80% of the river's measured discharge.

The chemical analyses of water samples that were collected at the same time of the flow-rate measurements provide the means to obtain mass-balance calculations for conservative solutes (excluding reaction sink–source terms). In particular, we have obtained such calculations for chloride, sulfate, and sodium using the following equation:

$$\frac{\partial(\forall \overline{C}^s_r)}{\partial t} = \sum_{i=1}^{n_{(in)}} Q_{in,i} C^s_{inlet} - \sum_{i=1}^{n_{(out)}} Q_{out,i} C^s_{r,i} + \int_{x_1}^{x_2} q_{in}(x) C^s_q(x)\mathrm{d}x - \int_{x_1}^{x_2} q_{out}(x) C^s_r(x)\mathrm{d}x \quad [4]$$

where C^s (mg L^{-1}) is the (cross-sectional average) concentration of solute s. The subscripts r, inlet, and q represent the river, inlets, and distributed ground water inflow, respectively, and an over-bar represents the segments' volume-average concentration. Using the assumptions of steady-state conditions $[\partial(\forall \overline{C}^s_r/\partial t = 0)]$, conservative elements, and zero distributed outflow $[\int_{x_1}^{x_2} q_{out}(x) C^s_r(x)\mathrm{d}x = 0]$, the total mass flow rate of the ground water contribution $[\int_{x_1}^{x_2} q_{in}(x) C^s_q(x)\mathrm{d}x$, referred to as $\dot{m}_{gw}$, g s^{-1}], is calculated. Table 4 shows the calculated mass flow rate of chloride, sulfate, and sodium in the river at Hamadia (Site 25, denoted as $\dot{m}_{25}$, g s^{-1}) based on the measured flow rate and chemical composition, of the ground water inflow [$\dot{m}_{gw}(N_2)$], and the ratio between them [$\dot{m}_{gw}(N_2)/\dot{m}_{25}$]. It is apparent that in most cases the ground water contribution is significant and that the chemistry of the river is indeed largely affected by the ground water discharge. The mass-balance calculations obtained for both N1 and N2 segments show that the river's sulfate discharge is increasing downstream while the chloride and sodium are decreasing. These calculations imply that the flow-weighted mean concentrations for all inputs are higher in the case of sulfate and lower in the case of chloride, relative to the concentrations of the river water.

Error Estimation

Although our instrumentation is considered highly accurate, and despite our detailed and careful measurement procedure, the mass-balance calculations contain some potential uncertainties. These uncertainties are due to possible errors in the velocity measurements and in the flow rate integration, in the reported pumping rates and estimated evapotranspiration (in particular the effective river width), in analytical error of the solutes concentrations, and due to potential deviations from the assumed steady-state conditions. To reduce errors generated by a possible non-steady-state condition, we coordinated our activities with the local authorities to limit sudden changes in the operation of the region water system. The only exception was an unavoidable release of fishpond drainage into the river during our measurement campaign in June. Although the average release discharge was provided, the June calculations may contain somewhat higher uncertainties. Because the discharge measurements were conducted during drought conditions, no significant natural variations are expected during all our measurement campaigns.

Deviations from steady-state conditions are potentially caused by variations in water level along the river

Table 4. Measured flow rates of chloride, sulfate, and sodium in the river, $\dot{m}_{25}$ (at Hamadia, Site 25), computed mass flow rates of the subsurface inflow in N_2 segment, $\dot{m}_{gw}(N_2)$, and their ratio, $\dot{m}_{gw}(N_2)/\dot{m}_{25}$

Period	Symbol	Cl	SO_4	Na
		g s^{-1}		
February 2001	$\dot{m}_{gw}(N_2)$	900	327	447
	$\dot{m}_{25}$	1656	510	808
	$\dot{m}_{gw}(N_2)/\dot{m}_{25}$	0.54	0.64	0.55
March 2001	$\dot{m}_{gw}(N_2)$	449	180	202
	$\dot{m}_{25}$	1673	482	772
	$\dot{m}_{gw}(N_2)/\dot{m}_{25}$	0.27	0.37	0.26
April 2001	$\dot{m}_{gw}(N_2)$	470	210	220
	$\dot{m}_{25}$	1330	374	641
	$\dot{m}_{gw}(N_2)/\dot{m}_{25}$	0.35	0.56	0.34
June 2001	$\dot{m}_{gw}(N_2)$	109	190	114
	$\dot{m}_{25}$	1939	465	928
	$\dot{m}_{gw}(N_2)/\dot{m}_{25}$	0.06	0.41	0.12
August 2001	$\dot{m}_{gw}(N_2)$	304	126	147
	$\dot{m}_{25}$	827	177	390
	$\dot{m}_{gw}(N_2)/\dot{m}_{25}$	0.37	0.71	0.38

segment, fluctuations of flow rates (in the river cross-sections, tributaries, drainage canals, and pumping stations), and temporal changes in solute concentrations. Assuming that the flow rates and concentrations are relatively steady within the time frame of the measurement campaign, the error analysis was based on the variations of water volume ($\forall$) alone. The change in water volume, $\partial\forall/\partial t$, was calculated using the following equation:

$$\frac{\partial \forall}{\partial t} = \int_{x_1}^{x_2} B(x)\frac{\partial h}{\partial t}(x)\mathrm{d}x \qquad [5]$$

where $B(x)$ (m) is the river's representative cross-section width (estimated from measurements at the discharge measurement sites) and $\partial h/\partial t(x)$ is the time derivative of water level during the measurement. Considering the minor influence of the relatively small water level fluctuations, $B(x)$ was assumed to be steady during the measurement period. The volume derivative was calculated assuming that the water surface is nearly linear, implying that the average $\partial h/\partial t$ represents the change in the entire segment.

Water levels were measured manually during the discharge measurements and automatically by electronic water level gages (equipped with data loggers) installed in June 2001. Because detailed water level measurements were performed only in July 2001, these measurements were used to estimate the water level changes in all the measurement campaigns. Changes of 1.25 and 0.63 mm h^{-1} were recorded at Sites 15 (width of 15 m) and 25 (width of 6.5 m), respectively. Using these values in Eq. [5] results in water volume changes of 90 and 20 L s^{-1} (in segment N2). The $\partial\forall/\partial t$ values obtained by manual water level measurements during the rest of the campaigns were approximately 90 L s^{-1}. Therefore, a 90 L s^{-1} value was used for the error estimation in N2 segment, with the exception of the June campaign. Due to the draining of the fishpond into the river (Site 20), a value of $\partial h/\partial t$ = 5 mm h^{-1} was recorded at Site 15, which corresponds to 155 L s^{-1}. This value was used for the June error estimation.

The calculated relative potential errors of the water discharge ($\Delta Q_{gw}/Q_{gw}$) and the solute discharge ($\Delta \dot{m}_{gw}/\dot{m}_{gw}$) are shown in Table 5. These potential errors represent the root mean square of all the possible errors generated by the terms in Eq. [3] and in Eq. [4]. As mentioned, the estimated relative errors of the measured flow rate are 5 to 6% for the river flow and 19 and 29% for the western and eastern tributaries. The potential error of the pumping rates was estimated as 20%, where the potential error of the evapotranspiration was estimated as 50%, due to the high uncertainty in the effective width, $B'(x)$. The relative error contributed by the $\partial\forall/\partial t$ term was 13 to 30% of the total calculated Q_{gw}, excluding the June campaign (where it corresponds to 80% of Q_{gw}). The error analysis of $\Delta\dot{m}_{gw}/\dot{m}_{gw}$ was obtained using the following estimates: the analytical error of the solutes concentrations was estimated as 5% (Farber et al., 2004); the potential error of the solute discharge at the inlets and outlets was calculated using a simple linear decomposition, $\Delta(QC) = C\Delta Q + Q\Delta C$; and the deviation from steady-state conditions, $\partial(\bar{C}_r^s\forall)/\partial t$, was evaluated assuming a constant $\bar{C}_r^s$. Table 5 shows the error estimates of the water, sulfate, and chloride discharge as calculated for each measurement campaign. With the exception of the June campaign, the error estimations of the calculated water discharge are 7 to 16% and those of solute discharge are 8 to 33%.

Table 5. Potential relative errors of the calculated water flow rates and calculated solutes mass flow rates of the subsurface inflow in N_2 segment. These errors represent the root mean square of all the potential errors of the terms in Eq. [3] and Eq. [4].

		February 2001	March 2001	April 2001	June 2001	August 2001
Water	$\Delta Q_{gw}/Q_{gw}$	0.07	0.16	0.13	0.34	0.14
SO_4	$\Delta\dot{m}_{gw}^{SO_4}/\dot{m}_{gw}^{SO_4}$	0.08	0.14	0.10	0.16	0.14
Cl	$\Delta\dot{m}_{gw}^{Cl}/\dot{m}_{gw}^{Cl}$	0.09	0.21	0.18	1.35	0.33

A Comparison between the Mass-Balance Results and the Geochemical Analysis

The concentration of dissolved constituents in the postulated ground water influx was calculated by dividing the mass flow rate of each of the solutes by the water volumetric flow rate, given that the assumption of zero distributed outflow holds. These calculations are used to compare the results of our mass-balance calculations with the results of the chemical analysis. The concentrations of chloride and sulfate in the ground water influx calculated for the different sampling campaigns are plotted in Fig. 4 together with measured concentration of river samples. Measured concentration of water samples that represent potential end-members such as fishponds, agricultural drainage, and tributaries are also included in Fig. 4. The data indicate that the computed composition of ground water, derived from the mass-balance calculations, is similar to the composition of the saline segment of the Yarmouk River (referred to as the "Saline Yarmouk").

Figure 4 shows that the samples taken from fishponds, western tributaries, and a shallow well on the west side of the river (named "Hamadia well") are not consistent with the linear river trend. Furthermore, the chemistry of eastern tributaries such as Wadi El Arab and Wadi Teibeh is outside the scale of Fig. 4 (having Cl < 800 mg L^{-1}). If the mixing process is limited to two distinct water bodies, the samples that were collected from the saline segment of the Yarmouk River (between Sites 9 and 11 [Fig. 1], referred to as the "Saline Yarmouk") and from some agricultural drainages can be considered as representing the end-members that affect the river chemistry.

Figure 4 shows that the concentrations of the calculated ground water source lie between the chloride and sulfate data points of the Saline Yarmouk River and those of the Lower Jordan River. These results are, in general, consistent with the geochemical evaluations that were made for the northern section of the Lower Jordan River (Farber et al., 2004). The agreement between the two studies greatly supports the conclusion that the northern part of the Lower Jordan River is

mainly affected by shallow ground water derived from agricultural drainages. The chemical composition of this end-member is similar but not identical to that of the Saline Yarmouk River, which in the geochemical study was assumed to represent the end-member composition. Whereas the geochemical evaluation is limited by the assumption of mixing between two sources, the results of the current study reflect the chemistry of the input to the river, which may be composed of multiple ground water sources with different geochemical end characteristics. These sources would have somewhat different compositions reflecting differences between the agricultural return flows of the west bank, the east bank, and additional inputs from deep ground water, local brines, and meteoric waters.

The Saline Yarmouk River constitutes a unique hydrological configuration that assists in the identification of the ground water influx to the Lower Jordan River. The Yarmouk River is dammed some 8 km east of its confluence with the Lower Jordan River and its water is diverted to the King Abdullah Canal (for the most part) and Yarmuchim Reservoir (Site 8, Fig. 1). Although no tributary inflow exists beyond the dam, the nearly zero flow rate at the dam increases significantly downstream toward the Yarmouk confluence point with the Jordan River. While the salinity upstream from the dam is low (140 mg Cl L^{-1}), the salinity of the downstream water is high (>1000 mg Cl L^{-1}). It should be noted that a pumping station at the end of the Saline Yarmouk River (Site 11), pumps most of the Saline Yarmouk surface water for fishery and irrigation usage. Hence, the direct inflow from the Saline Yarmouk into the Lower Jordan River is minimal, and therefore cannot have any impact on the water chemistry and flow rate of the downstream Lower Jordan River. Nevertheless, Fig. 4 shows that the geochemical signature of the Saline Yarmouk River is consistent with our mass-balance calculations and with the chemical modifications observed along the Lower Jordan River, both upstream and downstream from the confluence with the Yarmouk. Because the initial flow rate of the Saline Yarmouk is low, samples collected at Site 11 (Fig. 1) may represent the net effect of the subsurface sources that modify the chemistry of both the saline Yarmouk and the Lower Jordan River.

CONCLUSIONS

Our data show that at low flow rates of the northern section of the Lower Jordan River, the impact of natural ground water seepage and agricultural return flows is significant. By exercising a combination of careful discharge measurements, a complete account of inflows and outflows, and mass-balance calculations of both water and conservative constituents, we were able to characterize the distributed subsurface influx that affects the river water flow and chemistry. Subsurface flows are estimated to contribute 20 to 80% of the water discharge and 20 to 50% of the solutes discharge measured in two specific sections of the river (9.5 and 17 km long). It is noted that both the mass-balance calculations and the geochemical analysis cannot separate the influence of different sources (such as western and eastern ground water sources), thus the calculated source is likely to represent a mix of several end-members. To address this further, a campaign of multiple piezometer drilling is underway. These observation points will provide information regarding water levels and chemistry of the shallow ground water that flows to the Jordan River.

The future of the Jordan River was addressed in 1994 by the peace treaty between Israel and Jordan (Governments of Israel and Jordan, 1994). In the treaty, the two countries agreed to increase and equalize the overall pumping rights, to eliminate wastewater disposal into the river, and to use the saline water that currently flows into the river for desalination. The calculated impact of these steps, under the flow conditions reported here, shows that although water quality may improve, flow rates in some of the river segments will decrease to a level that will dry the river. The authorities of both countries must address this unsolved problem.

ACKNOWLEDGMENTS

The study was supported by the U.S. Agency for International Development, the Middle East Regional Cooperation Program (MERC Project M20-068), by the Grand Water Research Institute (Technion), and by the Joseph & Edith Fischer Career Development Chair. We also thank ECO Jordan, the Palestinian Hydrology Group, the Israeli Nature Protection Authority, and the local water and agricultural authorities for their logistic support.

REFERENCES

Al-Washah, R.A. 2000. The water balance of the Dead Sea: An integrated approach. Hydrol. Processes 14:145–154.

Benjamin, M.M. 2002. Water chemistry. McGraw-Hill, Boston.

Coleman, M.L., and M.P. Moore. 1978. Direct reduction of sulfates to sulfur-dioxide for isotopic analysis. Anal. Chem. 50:1594–1595.

Efrat, E. 1996. The land of Israel—Physical, settlement and regional geography. Tel-Aviv Univ., Israel.

Farber, E., A. Vengosh, I. Gavrieli, A. Marie, T.D. Bullen, B. Mayer, R. Holtzman, M. Segal, and U. Shavit. 2004. Hydrochemistry and isotope geochemistry of the Lower Jordan River: Constraints for the origin and mechanisms of salinization. Geochim. Cosmochim. Acta 68:1989–2006.

Gavrieli, I., Y. Yechieli, L. Halicz, B. Spiro, A. Bein, and D. Efron. 2001. The sulfur system in anoxic subsurface brines and its implication in brine evolutionary pathways: The Ca-chloride brines in the Dead Sea area. Earth Planet. Sci. Lett. 186:199–213.

Governments of Israel and Jordan. 1994. Israel–Jordan Peace Treaty. Annex II, water and related matters [Online]. Available at www.mfa.gov.il/MFA/Peace+Process/Guide+to+the+Peace+Process/Israel-Jordan+Peace+Treaty+Annex+II.htm (verified 8 Dec. 2004). Governments of Israel and Jordan.

Hamberg, D. 2000. Flows in the Lower Jordan River. Report for the Office of National Foundation. 6130-d00.385. Tahal, Israeli Water Div. Office, Israeli Office of National Foundation, Tahal, Tel-Aviv, Israel.

Hof, F.C. 1998. Dividing the Yarmouk's waters: Jordan's treaties with Syria and Israel. Water Policy 1:81–94.

Holtzman, R. 2003. Water quality and quantities along the Jordan River—Salinization sources and mechanisms. (In Hebrew; tables, figures, and references in English.) M.S. thesis. Technion-Israel Inst. of Technology, Israel.

Hvitved-Jacobsen, T. 2002. Sewer processes: Microbial and chemical process engineering of sewer networks. CRC Press, Boca Raton, FL.

Marsh-McBirney. 1990. Model 2000 installation and operations manual. Marsh-McBirney, Frederick, MD.

Orthofer, R., R. Daoud, B. Fattai, M. Ghanayem, J. Isaac, H. Kupfers-

berger, A. Safar, E. Salameh, H. Shuval, and S. Wollman. 2001. Developing sustainable water management in the Jordan Valley. Joint synthesis and assessment report. Final report to the European Community. ERBIC18CT970161. Austrian Res. Centers, Vienna.
Pillsburry, A.F. 1981. The salinity of rivers. Sci. Am. 245:54–65.
Salameh, E. 1996. Water quality degradation in Jordan: Impacts on environment, economy and future generations resources base. Friedrich Ebert Foundation and Royal Soc. for the Conservation of Nature, Amman, Jordan.
Salameh, E., and H. Naser. 1999. Does the actual drop in Dead Sea level reflect the development of water resources within its drainage basin. Acta Hydrochim. Hydrobiol. 27:5–11.
Segal-Rozenhaimer, M., U. Shavit, A. Vengosh, I. Gavrieli, E. Farber, R. Holtzman, B. Mayer, and A. Shaviv. 2004. Nitrogen pollutants, sources and processes along the Lower Jordan River. J. Environ. Qual. 33:1440–1451.
Sontek. 2000. Sontek technical notes. Argonaut ADV principle of operation. Sontek, San Diego, CA.
Williams, W.D. 2001. Anthropogenic salinization of inland waters. Hydrobiologia 466:329–337.